INTRODUCTION OF 300MW FUEL ASSEMBLY SPACER GRID IMPROVEMENT IN QINSHAN PHASE-I NPP

LIBING ZHU[1], FUJUN GAN[1], JIE DING[1], YUNQING ZHOU[1]

[1] *Shanghai Nuclear Engineering Research & Design Institute, 29# Hongcao Road, Shanghai, China, 200233*

Abstract: The FA300 fuel assembly, which was first developed by Shanghai Nuclear Engineering Research and Design Institute (SNERDI), has been commercially used since 1991. Up to now, more than 1500 assemblies have been discharged from Qinshan phase-I and Pakistan Chashma C1-C4 NPPs. Based on the feedbacks from the above utilities, SNERDI has been carrying out continuous design improvements on the FA300 fuel assembly. The newest generation was mainly focused on the spacer grids, to reduce the potential hang up damage risk during refueling operation. New design of guide vanes was added to decrease the possibility of snag event between two fuel assemblies. In the whole project, a series of tests and analysis has been carried out to demonstrate that the mechanical and thermal-hydraulic performance of new designed grid can meet pre-determined functional and safety requirements. After that, fuel assemblies with new spacer grids were approved to be loaded into Qinshan phase-I reactor. Until now, these FAs have experienced one cycle, and behave very well during the refueling processes.

1. Introduction

The 300MW NPP fuel assembly (FA300) , which was first developed by Shanghai Nuclear Engineering Research and Design Institute (SNERDI), has been commercially used since 1991. Up to now, more than 1500 assemblies have been discharged from the reactor in Qinshan phase-I and Chashma C1-C4 NPPs. During these 27 years, SNERDI has been carrying out continuous design improvements on the fuel assembly based on the feedbacks from utilities, to enhance Safety, reliability and economics of the reactor and fuel assemblies. Table 1 shows the main three stages during the whole improvement process of FA300, including the cladding material optimization to improve the burnup capability, the debris filter design to minimize the leaking rate of fuel due to debris fretting, and the anti-snag grid design to enhance the reliability during refueling operations.

Table 1　Upgrade history of FA300 fuel assembly

	FA300-1	FA300-2	FA300-3	FA300-3+
Design finished	1985	1996	2001	2016
First used	1991	1999	2003	2017
Main design features	1.Conventional Zr-4 cladding 2.Stainless steel guide thimble 3. Nickel base alloy spacer grid	Optimal low Tin cladding	Debris filter in bottom nozzle Chamfer on the pellet The allowable acceleration exerted on the fuel assembly increase to 4.0g	Anti-snag grid

Although the operation history was very good during the past three decades, lots of hanging up events happen during the refueling process, which is mainly due to unreasonable design of spacer grid guide vanes. Figure 1 shows that one of the lower guide vanes was damaged when the neighboring fuel assembly was lifted up. Hanging up damage to fuel assemblies not only makes refueling period become longer but also is adverse to the safe operation for fuel assemblies in following cycles.
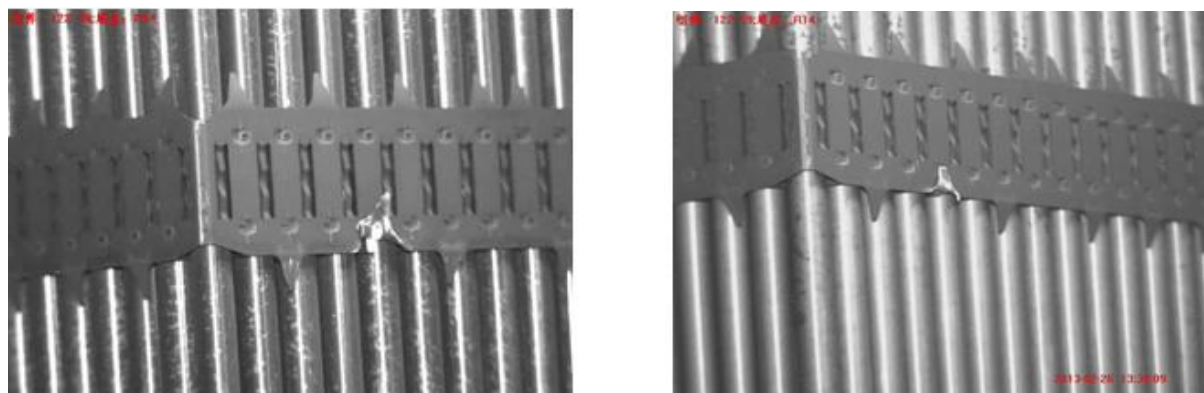

Fig.1　Pictures of damaged spacer grids during refueling

In order to reduce potential hanging up damage risks, SNERDI carried out a project to optimize the spacer grid guide vanes, and the target of the project is usage of fuel assemblies with new guide vanes in following cycles of Qinshan phase-I reactor. The whole project includes re-design of guide vanes and pre-analysis of mechanical, thermal-hydraulic performance of new spacer grid, test articles manufacture and final performance validation via different tests.

Figure 2 and 3 are sketches of old and new spacer grid designs of FA300 fuel assembly, respectively. Comparing with the new design, the number of guide vanes is much less for both upper and lower guide vanes, and the shape is much sharper, which may enhance the hanging up risk. For this improvement, series of hanging up tests were carried out, demonstrating that hardly any snag event happed during the whole test processes.

In addition to validation of hanging up performance of new spacer grids, more attentions should be focused on influences of the new designed guide vanes on thermal-hydraulic performance.
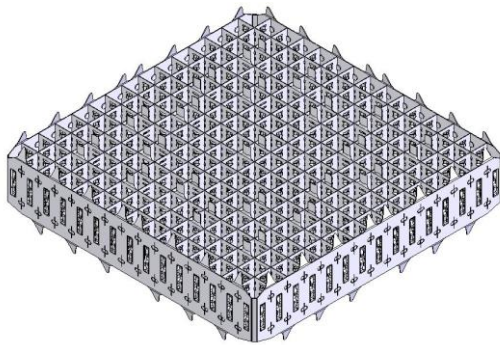

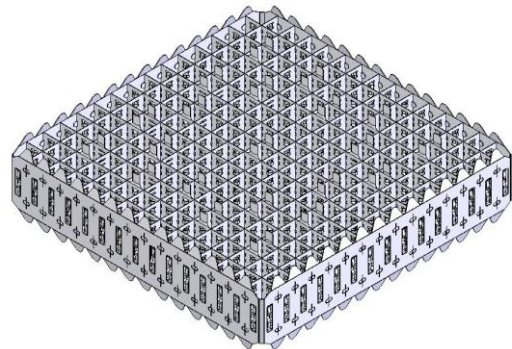Fig.2　Original spacer grid design　　　　Fig.3　Improved spacer grid design

2. Hanging up tests

Snag behavior would damage FA spacer grid, which will affect fuel safety and degrade its economy. The goal of the hanging up test was verify that the FA can prevent itself from snagging with adjacent FAs. A series of out-of-pile tests have been carried out in out-reactor conditions to simulate limiting situations that would occur between fuel assemblies during the refueling process, as shown is Figure 4.
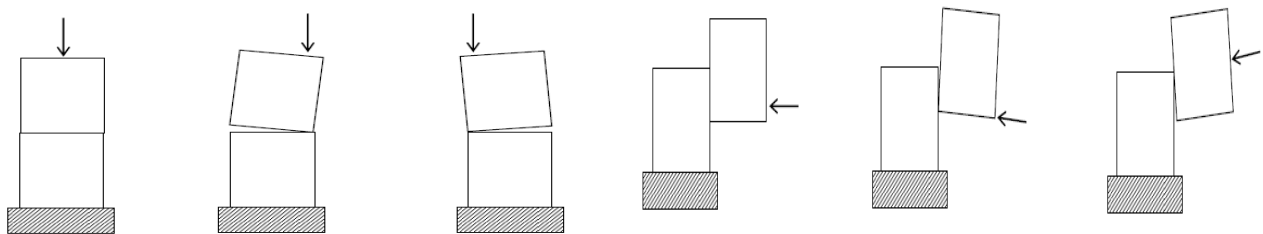

Fig.4　Schematic sketches of series hanging up tests

Tests were carried out on a specific test stand up, as is shown in Figure 5. Hoisting a fuel assembly to simulate the fuel handling operation, meanwhile applying a lateral force on the FA to make it contact with anther FA which is fixed on a test stand. Nine kinds of contact situation between two adjacent assemblies are considered. Hanging up due to the fuel assembly bow is not

included because no obvious fuel bow has been observed Tests were carried out at a low and a high hoisting speed to simulate different operation modes. All cases are repeated up and down operations 3 times. Results show that, when using the old design, snag occurs 81 times during the experiment, corresponding to a relative snag risk 6.8%. While using the new design, no snag occurs during the experiment , corresponding to a relative snag risk 0.0%. Figure 6 show the pictures of destroyed old spacer grid and well behaved new spacer grid. Obvious damage was observed for the old spacer grids during tests.
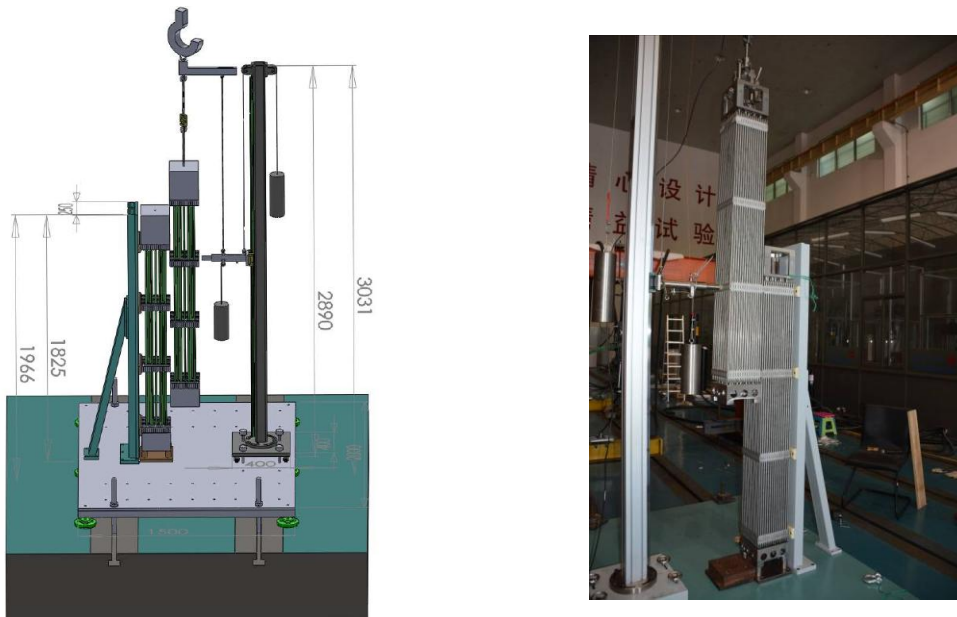

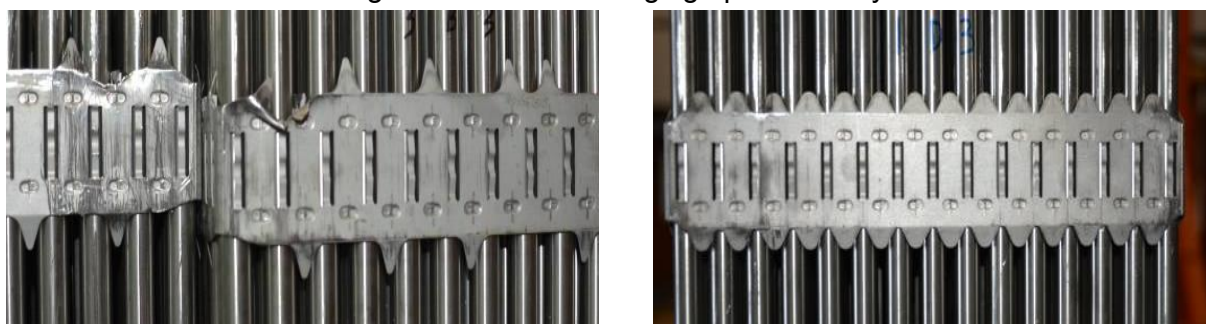Fig.5　sketches of hanging up test facility

Fig.6　Original spacer grid design

3. Thermal-hydraulic analysis and tests

In addition to validation of hanging up performance of the new spacer grid, more attention was focused on the influence of the new designed guide vane on thermal-hydraulic performance. Additional work has been finished to make sure that, enough DNBR margin was maintained, including qualitative comparison of the flow field and heat transfer phenomena in fuel rod bundles

under the effect of old and new spacer grid, respectively, to make sure the very conservative W-3 correlation was still applicable. Pressure drop tests were also carried out to obtain the loss coefficient of old and new 15×15 spacer grids. Together with the ratio of sub-channel grid loss coefficient calculated with the help of commercial CFD software STAR-CCM+, the important input parameters of DNBR analysis, i.e. loss coefficient of typical, thimble, side and corner sub-channels, were obtained. Finally, DNBR analysis and comparison were finished, demonstrating hardly effect of new designed spacer grid guide vane on the core thermal-hydraulic performance.

3.1   Applicability evaluation of W-3 correlation using CFD method

In order to compare the core DNBR margin under the effect of fuel assemblies using old and new spacer grid, the applicability evaluation of the W-3 correlation in NCED code (sub-channel code) should be conducted at first, though the W-3 correlation is very conservative. Qualitative CFD comparison was employed instead of quantitative analysis, such as CHF test, CFD simulations were performed aiming to compare the flow field characteristic and heat transfer phenomena in fuel rod bundles under the impact of old and new spacer grid, respectively.
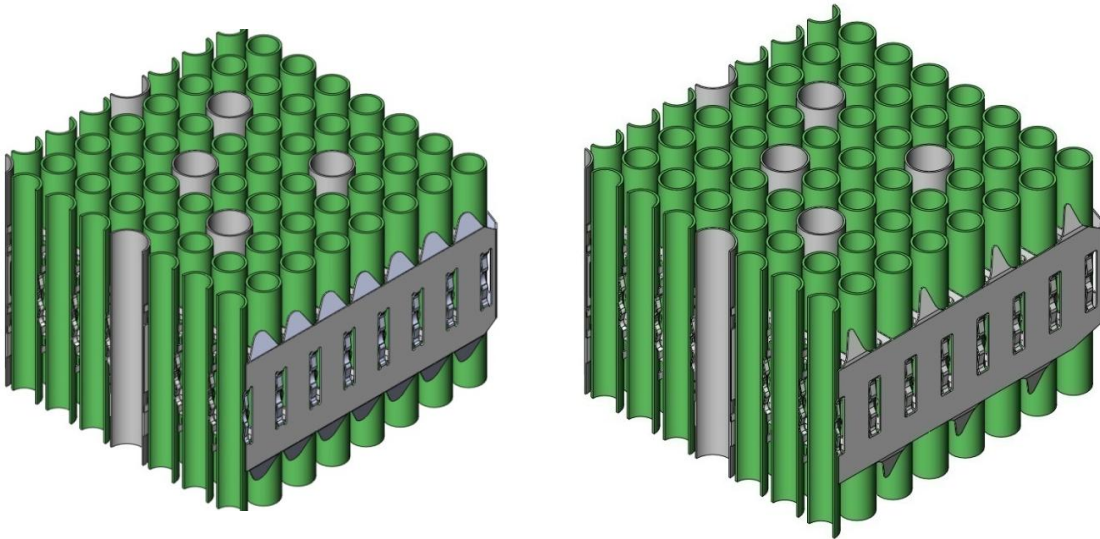

Fig.7   Schematic of the computational model

The computational model is a span of typical 15×15 FA300 grid, as shown in Figure 7. Above CFD model contains all detailed structures including grid straps, springs, dimples, mixing vanes and welding spots, which is the same as grids used in tests. Thickness of the grid and fuel cladding are considered. The axial domain covers from 10 D_h upstream of the grid to about 55 D_h downstream of the grid. The upstream section is set to allow the coolant flow to be fully developed before reaching the midgrid. The downstream section covers the span length between two

adjacent mid-grids. The radial domain only contains a quarter of the grid due to the geometrical symmetry.

Polyhedral mesh and embedded thin mesh are used in the fluid region and solid region, respectively. The base size is 0.3325mm, minimum mesh size is 25% of base size. The fluid physics model is three dimensional steady-state single phase water with constant density, the solid physic model is three dimensional steady state, the material is Zr with constant density. Realizable two-layer k-epsilon turbulence model with all y+ wall treatment is employed.

The boundary conditions for the CFD model are obtained from the Final Safety Analysis Report of Qinshan phase-I NPP. Uniform velocity and temperature are specified at the inlet, the reference pressure equals the core exit pressure. No-slip conditions are applied for all the walls. Constant heat fluxes are applied to the inner surface of each rod, which is based on the core average power and the total heated length. The rotational periodic boundary conditions are applied to the four sides of the CFD domain.

Figure 8 show the lateral velocity distribution of fluid region at a given elevation. The difference of original model and improved model mainly exist in the region near the guide vane. The two central vortexes in the sub-channel near the guide vane in the original model are round, and flow in opposite direction, while the central vortexes in the sub-channel near the guide vane in the improved model are elliptical. The vortexes dissipate over distance. At y=160 mm, the vortexes in the original model disappear and a regular perturbation around each side fuel rod is formed. While for the improved model, a regular semicircular vortex is formed in the center of the sub-channel. The lateral flow in the other regions is basically the same in the original model and improved model.
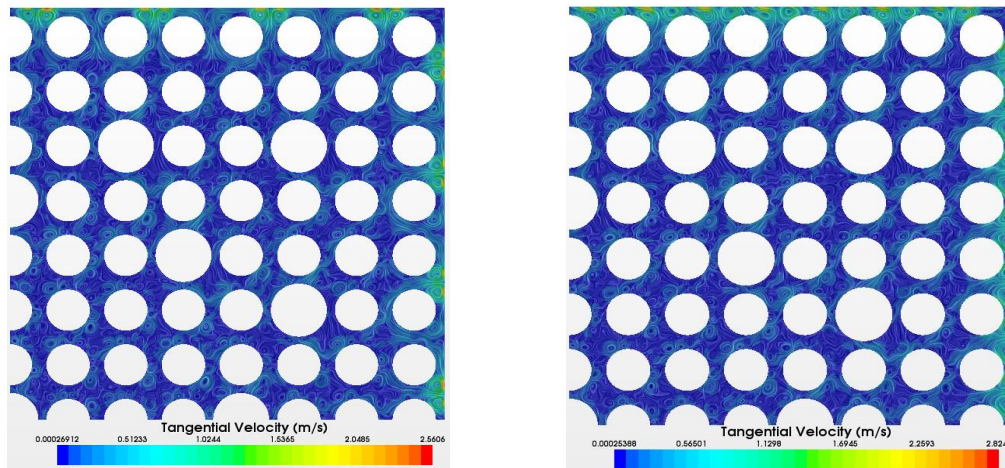
(a) Orignial   (b) Improved

Fig.8 Lateral velocity distribution of fluid region (y=10 mm)

Figure 9 shows the total temperature comparison. The temperature range for rods under the effect of the original grid is 575.15 K~599.88 K, the temperature range for rods under the effect of improved grid is 575.15 K~599.45K, which indicated that the modifying the structure of the guide vane does not influence the rod surface temperature range. Figure 10 and 11 compare the maximum temperature axial distribution and radial distribution of the rod in the middle of the bundle. It can be seen that the maximum temperature distribution is basically the same in the original model and improved model. The position of the maximum temperature locates at the same region, and the temperature range is the same, the difference of the maximum temperature is only 0.2 K.

(a) Orignial   (b) Improved
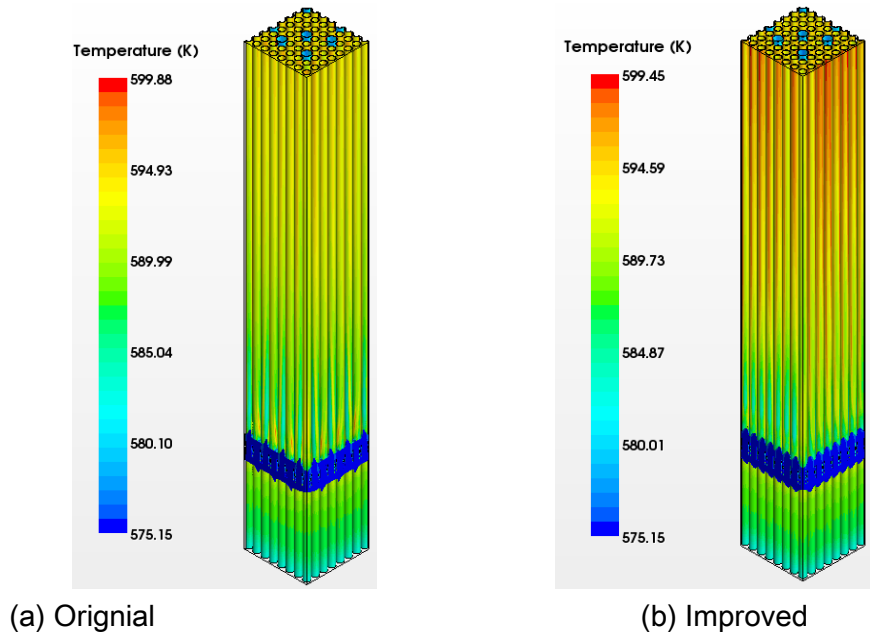
Fig.9 Total rod surface temperature distribution
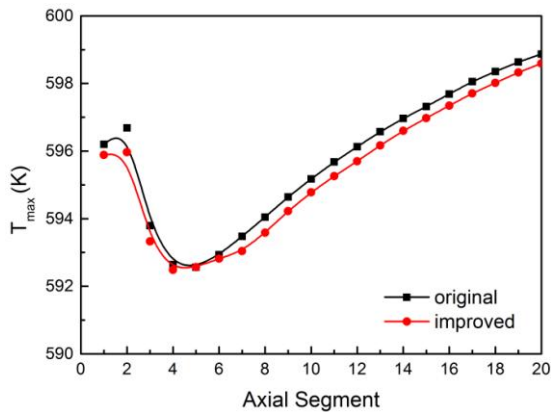

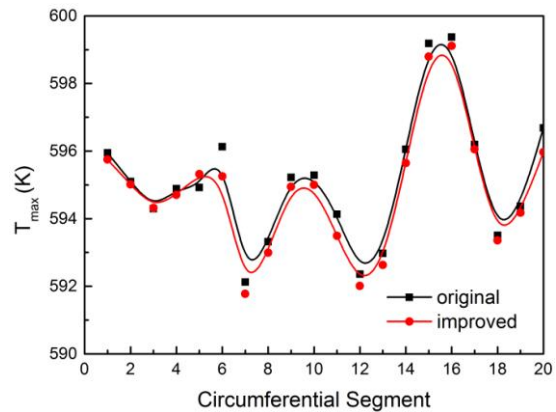Fig.10   Axial distribution of rod maximum temperature downstream of spacer grid

Fig.11   Radial distribution of rod maximum temperature downstream of spacer grid

Above CFD simulations show that the difference of loss coefficient between old and new spacer grid is 0.081, which is almost the same as the value obtained from tests. The flow field and temperature distribution are almost the same, demonstrating that the impact of the new spacer grid guide vane can be neglected.

3.2   Pressure drop tests of 15X15 fuel assemblies

To determine the loss coefficient of a sub-channel grid, the loss coefficient of the whole grid is necessary as well as the ratio of loss coefficient of different sub-channels. Thus, two 15×15 short fuel assemblies shown in Figure 12 were designed and produced; one consists of 4 old spacer grids, and the other 4 new spacer grid. These test assemblies were put into a square flow housing, shown in figure 13, to measure the pressure drop of interesting sections, and finally get the fitting correlations between test Reynolds number and grid loss coefficient, as is shown in figure 14. Results show that, the loss coefficient of new spacer grid is 0.77, a little higher than the old design, as is shown in Figure 14.
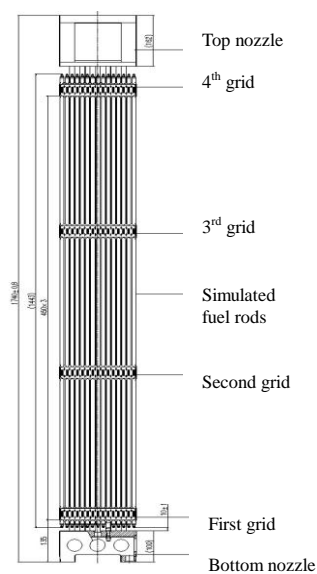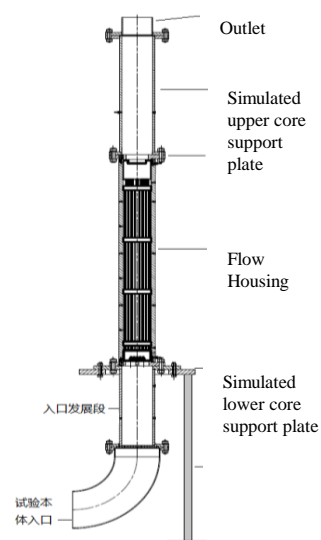

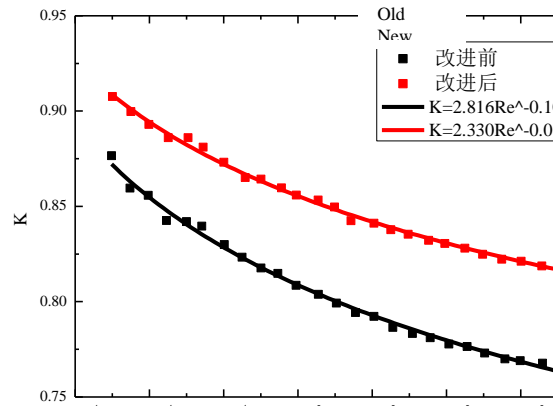Fig.12   Sketch of test article   Fig.13   Sketch of flow housing

Fig.14 Fitting curve of loss coefficient of grid

3.3　　　Calculation of ratio of sub-channel grid loss coefficient

Based on the experimentally determined loss coefficient of the whole 15×15 grid, it is easy to calculate the loss coefficient of each type of sub-channel. Figure 15 shows the schematic of the sub-channel, the definition of sub-channel is the same as the subsequent DNBR calculation. There are four kinds of sub-channel in FA300 grid, including typical, thimble, side and corner sub-channel.

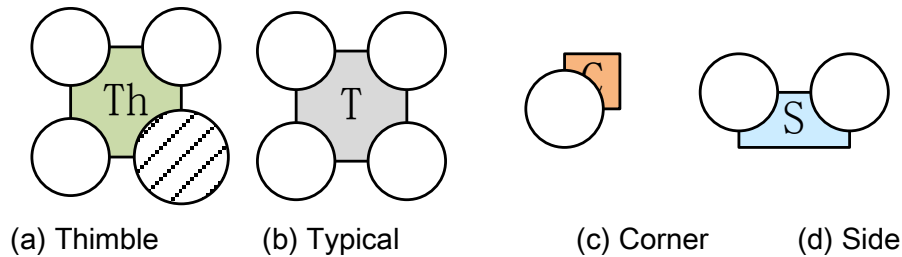(a) Thimble　　　(b) Typical　　　(c) Corner　　(d) Side

Fig.15　Schematic of different sub-channels

An analytical method has been developed for evaluating the ratio of the sub-channel loss coefficient based on the experimentally determined grid loss coefficient. The method is based on the flow conservation equation,

$$Q = N_{Th}Q_{Th} + N_S Q_S + N_C Q_C + N_T Q_T$$

Where Q is the volumetric flow rate in the fuel rod bundle, Q_{Th}、Q_T、Q_S and Q_C represent the flow rate in single thimble sub-channel, typical sub-channel, side sub-channel and corner sub-channel, respectively. N_{Th}、N_T、N_S and N_C represent the number of thimble sub-channels, typical sub-channels, side sub-channels and corner sub-channels, respectively.

The total pressure drop of the grid region , includes the pressure loss due to the grid loss and the friction loss of the fuel rod:

$$\Delta p_{grid} = \frac{1}{2}\rho V^2 \left(k_0 + \frac{fL}{D_h} \right) = \frac{1}{2}\rho \left(\frac{Q}{A} \right)^2 K$$

The following equation can be obtained by combing the above two equations:

$$\frac{A}{\sqrt{K}} = \frac{N_{Th}A_{Th}}{\sqrt{K_{Th}}} + \frac{N_S A_S}{\sqrt{K_S}} + \frac{N_C A_C}{\sqrt{K_C}} + \frac{N_T A_T}{\sqrt{K_T}}$$

Where K_{Th}、 K_T、 K_S and K_C represent the loss coefficient of single thimble sub-channel, typical sub-channel, side sub-channel and corner sub-channel, respectively.

The present work constructs four CFD computational models, as is shown in Figure 16. Model 1 contains four thimble sub-channels Model 2 contains 4 thimble sub-channels and 12 typical sub-channels. Model 3 contains 4 corner sub-channels. Model 4 contains 4 corner sub-channels, 8 side sub-channels and 4 typical sub-channels. Based on the above equations, loss coefficient of each type of sub-channel can be obtained. The mesh size, mesh type, boundary condition and physical models are the same to the previous 15×15 FA300 full-scale CFD simulation. The CFD results show the K_{Th}, K_T、 K_S and K_C of original grid is 0.7, 0.72, 0.72 and 0.67, the K_{Th}, K_T、 K_S and K_C of improved grid is 0.69, 0.71, 1.59 and 0.66.
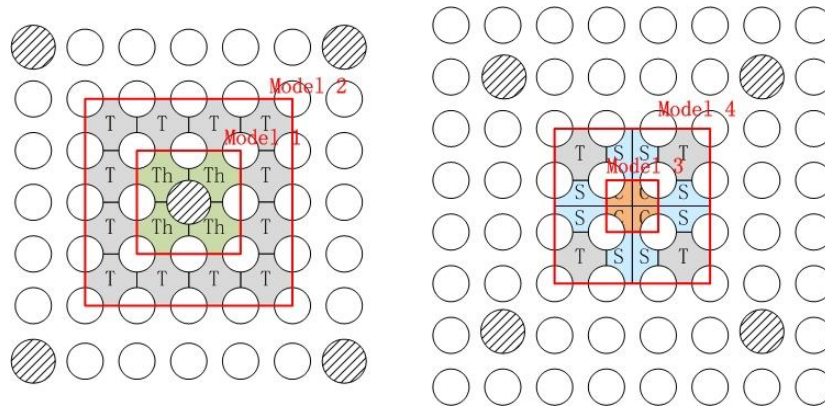

Fig.16   Schematic of the CFD models

3.4   DNBR analysis

Based on a safety analysis 14 sub-channel model, modifying the hot fuel assembly position to the corner of four assemblies, a side-cornel sub-channel model of 300MW NPP was established, which can directly model the typical channel, the thimble channel, the side channel and the corner channel. The radial power distribution of sub-channel analysis was also modified to make the side and corner cell the hot cell, which can make sure the model was conservative for safety analysis.

The Qinshan Final Safety Analysis Report indicates the Minimum DNBR of Qinshan 300MW NPP is 1.94. From table 1, after the improved FA300 is loaded in Qinshan 300MW NPP, the minimum DNBR is 1.93, which is a little lower than FSAR result. The penalty of DNBR is no more than 1%. But the actual Qinshan 300MW NPP power is 966MW and average temperature of coolant is 295℃. If any one factor of power and average temperature is considered during the calculation, 5% more DNBR margin can be obtained. If power and average temperature are are considered simultaneously, 11% more DNBR margin can be obtained.

So if considering the real operation core average temperature or core thermal power of 300MW NPP, the DNBR result of FSAR can be bounded by the side and corner sub-channel analysis.

Table 1 Comparison of Min DNBR.

	Power (MWt)	Coolant T (K)	Min DNBR
Old Fuel assembly	1035	575.12	1.94
New fuel assembly	1035	575.12	1.93

4. Conclusion

Based on the feedbacks from utilities, SNERDI has been carrying out continuous design improvements on the fuel assembly. The last improvement was focused on the guide vanes on the outer straps of spacer grid , to reduce the potential hang up damage risk during refueling operation. New guide vanes were added to decrease the possibility of a snag event between two fuel assemblies.

During the whole project, multiple tests and analysis were carried out to demonstrate that the mechanical and thermal-hydraulic performance of new designed grid can meet pre-determined functional and safety requirement. After that, fuel assemblies with new spacer grids were approved to be loaded into Qinshan phase-I reactor. And the feedback from the utility has been very good during refueling processes.